frontiers | Frontiers in Materials

TYPE Original Research
PUBLISHED 06 January 2023
DOI 10.3389/fmats.2022.1109363

OPEN ACCESS

EDITED BY
Kezhen Qi,
Shenyang Normal University, China

REVIEWED BY
Shunru Zhang,
Huaihua University, China
Hongxiang Wang,
Shandong University, China

*CORRESPONDENCE
Hongjuan Sun,
sunhongjuan@swust.edu.cn

SPECIALTY SECTION
This article was submitted to Environmental Degradation of Materials, a section of the journal Frontiers in Materials

RECEIVED 27 November 2022
ACCEPTED 19 December 2022
PUBLISHED 06 January 2023

CITATION
Yang H, Guo H, Sun H and Peng T (2023), Surface modification study of CaO-Al_2O_3-SiO_2-Fe_2O_3 base system high temperature phase reconstruction.
Front. Mater. 9:1109363.
doi: 10.3389/fmats.2022.1109363

Surface modification study of CaO-Al_2O_3-SiO_2-Fe_2O_3 base system high temperature phase reconstruction

Huanyin Yang[1,2], Hongli Guo[2], Hongjuan Sun[1,4]* and Tongjiang Peng[1,3,4]

[1]Key Laboratory of Solid Waste Treatment and Resource Reuse, Ministry of Education, Southwest University of Science and Technology, Mianyang, Sichuan, China, [2]College of Electronic and Information Engineering, Yangtze Normal University, Fuling, Chongqing, China, [3]Analysis and Testing Center of Southwest University of Science and Technology, Mianyan, Sichuan, China, [4]Institute of Mineral Materials and Applications, Southwest University of Science and Technology, Mianyang, Sichuan, China

The fly ash was used as raw material to prepare glass ceramic base body, on which a layer of glaze slurry was applied, then, the complex was successfully prepared by sintering at 1180 °C through single-sinter process. Influences of quartz sand content on crystal phase evolution, physical–mechanical properties, and surface morphology of products were studied systematically. Finally, an opaque glaze with 15 wt% quartz sand fitting on glass ceramic base body had been produced, exhibiting a unique main phase, mullite, which ensured a significant Vickers microhardness of 8.1 GPa, improving the mechanical properties of solid waste glass ceramic base body. It was also found that the water absorption of the product was .66%, which greatly enhanced the waterproof function of the base surface. The complex products developed in this study were expected to be used as building decoration materials and provided new ideas for effective reuse of other similar solid wastes.

KEYWORDS

fly ash, glaze, phase reconstruction, surface modification, solid wastes

1 Introduction

Fly ash (FA) is a kind of solid waste produced in the process of coal combustion in thermal power plants. Millions of tons of FA are produced in thermal power generation in China every year, most of which are mainly stored, causing pollution to the surrounding soil and rivers and ecological damage. With the increase of annual coal power consumption and the potential serious threat of fly ash to the environment, the resource utilization of fly ash has been studied at home and abroad (Iyer and Scott, 2001; Dong et al., 2009; Fernandes et al., 2009; Zhao et al., 2010; Zhang et al., 2020; Ali et al., 2021; Gao et al., 2021), involving fields such as cement, concrete admixture, cementable materials, wall materials, wastewater treatment agents, soil amendments, roadbed materials, *etc.* FA mainly composed of SiO_2, Al_2O_3, CaO, Fe_2O_3 and other chemical components, is suitable for the preparation of CaO-Al_2O_3-SiO_2-Fe_2O_3 glass-ceramics. In recent years, a large number of studies have been carried out on the preparation of glass-ceramics by high-temperature phase reconstruction with fly ash as the main raw material (Barbieri et al., 1999; Albertini et al., 2013; Guo et al., 2014; Wang et al., 2014; Zhu et al., 2016). Due to the influence of fly ash components, most of the research focuses on adding other minerals or chemical raw materials to fly ash to achieve the excellent performance of products. Yang used fly ash and blast furnace slag as the main raw materials to prepare waste slag glass-

TABLE 1 Chemical analysis determined by XRF of industrial waste: fly ashes (FA) (wt%).

SiO_2	Al_2O_3	CaO	MgO	K_2O	Na_2O	ZnO	Fe_2O_3	TiO_2	BaO	ZrO_2	P_2O_5	MnO	SrO	Others	SO_3
39.13	16.74	7.70	0.33	2.91	0.28	0.07	22.97	5.25	0.16	0.33	0.44	0.17	0.26	-	3.01

ceramics by direct sintering method, and discussed the influence of fly ash content on the crystalline phase composition and properties of glass-ceramics (Yang and Zhang, 2015). Li prepared the glass ceramics of CaO-Al_2O_3-MgO-SiO_2 system with fly ash and Bayan Obo tailings as the main raw materials, and tested the physical and mechanical properties of the prepared glass ceramics (Li et al., 2013). The results showed that the glass ceramics have broad prospects for construction and application. Lu used glass and fly ash, added 10% magnesium oxide to prepare glass-ceramics by direct sintering method, which exhibited the main crystal phase of pyroxene and magnesia olivine (Lu et al., 2016). The product had the characteristics of high strength and low density, and was suitable for building materials. Above all, there are many researches on the preparation of glass ceramics by solid waste (Shang et al., 2021; Zhang et al., 2022), but there is no report on the preparation of glass ceramics by fly ash only.

In view of the shortcomings of fly ash glass-ceramics such as large porosity, poor surface finish and deep color, which limited its application. Therefore, the surface of the glass ceramic body was modified by glazing. At present, the researches of ceramic glaze slurries mainly focuse on that the slurries are applied on the sintered ceramic substrate, and then are secondary sintered, which is greatly affected by the atmosphere. In this paper, CaO-Al_2O_3-SiO_2-Fe_2O_3 system glass-ceramic was prepared from fly ash, and an opaque glaze slurry was applied on the glass-ceramic green body. The product was successfully prepared by one-time sintering without being affected by the atmosphere, which can save energy consumption and production cost. The study provides a new way for improving the properties of the FA glass-ceramic, promoting its industrial scale as a common decorative material, and the bulk resource utilization of fly ash.

2 Experiment

2.1 Sample preparation

Green body:Flash ash from a place in Sichuan was selected as raw material, its chemical composition was shown in Table 1, and was pressed into shape by a tablet press (d = 2 cm). Part of which is used as glaze substrate, and part is sintered together with glazed samples in the furnace. The sintered body is named SFA.

The raw glaze slurry:The minerals such as Kaolin, potassium feldspar, wollastonite, quartz sand, fired talc and commercial grade calcium phosphate, zinc oxide were selected as raw materials, of which chemical compositions are given in Table 2. On the basis of the previous work, the raw glaze slurries with different quartz sand content were prepared by mixing 5wt% kaolin, 45wt% potassium feldspar, 14wt% wollastonite, 5wt%-20wt% quartz sand (QS), 10wt% fired talc, 3wt% ZnO (calcined), 8wt% $Ca_3(PO_4)_2$ with 0.8wt% sodium carboxyl methyl cellulose (CMC) and .3 wt% sodium tripolyphosphate (STPP) according to the material: ball: water = 1:2:0.75 in a ball mill at a rate of 750 r/min for 30min. Then the raw glaze slurries were applied to the green bodies (d = 2 cm) by brushing. After dried, the samples were fired at a heating rate of 5 °C/min to 1180°C, and then sintered for 30 min at this temperature. Finally, the samples were cooled down to room temperature naturally in the furnace. The sintered samples with different quartz sand contents labeled GFA1-GFA4 are listed in Table 3.

2.2 Characterization

The chemical compositions of FA and glaze raw materials were determined by X-ray fluorescence spectroscopy (XRF, Axios, PANalytical, Netherlands). The phase and the crystal structure of the sintered samples were detected *via* X-ray diffraction (XRD, D/MAX- IIIB, Rigaku, Japan). Scanning electron microscopy (SEM, Ultra55, Zeiss, Germany) was employed to observe the microscopic morphology of the sintered samples. Using a digital camera to observe the surface morphology of the sintered complex. The water absorption of the sintered samples was determined according to the Archimedes' principle by the boiling method, and calculated by using the following expression:

$$w = \frac{m_1 - m_0}{m_0} \times 100\%,$$

where m_0, m_1 and w represent the dry weight of the sample in air, the mass of the water-saturated sample in air and the water absorption, respectively.

A micro-hardness tester (HV-1000A, Laizhou Huayin Testing Instrument Co., Ltd. China) was used to measure the Vickers hardness of the sintered samples under the condition that a load of 500 g was applied for 30 s to scratch their surfaces. At least five scratches were made on each sample to obtain reliable data.

3 Results and discussion

3.1 Characterization of raw materials

Erol M. used FA from different origins as raw material to prepare glass ceramics by direct sintering, and found that the chemical composition and particle size distribution of FA had a great influence on the property of glass ceramics (Erol et al., 2008). It is well known that SiO_2 and Al_2O_3 serve to form the glass network and are essential for the synthesis of glass ceramics. The property of glass ceramics with higher Al_2O_3 and SiO_2 content was better. In this study, FA composed of lower Al_2O_3 and SiO_2 content may lead to poor surface properties of the samples. The higher Fe_2O_3 content in FA may lead to the dark color.

Figure 1 shows the XRD pattern of FA. A noticeable hump can be observed for the amorphous silicate glass, which is due to the high-temperature carbonized process. Besides, several obvious diffraction characteristic peaks are also observed, which are quartz (PDF # 00–046–1045, SiO2), mullite (PDF # 00–015–0776, $Al_6Si_2O_{13}$) and hematite (PDF # 00–001–1053) respectively. This indicates that FA is

10.3389/fmats.2022.1109363

TABLE 2 Chemical analysis determined by XRF of glaze raw materials (wt%).

	SiO_2	Al_2O_3	CaO	MgO	K_2O	Na_2O	ZnO	Fe_2O_3	TiO_2	BaO	ZrO_2	P_2O_5	MnO	SrO	Others	SO_3
Kaoline	54.82	38.19	1.38	-	0.30	0.19	0.01	1.31	3.16	-	0.21	-	-	-	0.04	0.39
Feldspar	62.08	10.54	1.13	-	22.10	0.31	0.02	1.05	-	1.07	0.23	0.12	0.10	0.24	1.01	-
Fired Talc	81.96	0.29	5.75	10.21	-	0.11	-	0.69	-	-	-	0.48	-	-	0.51	-
wollastonite	51.75	-	48.25	-	-	-	-	-	-	-	-	-	-	-	-	-
Quartz	99.21	0.24	0.12	0.06	0.07	0.10	-	0.05	-	0.02	0.00	-	-	-	0.19	0.02

TABLE 3 The weight ratio (wt%) of quartz sand in different samples.

	Quartz sand other	Raw materials
GFA1	20	same
GFA2	15	same
GFA3	10	same
GFA4	5	same

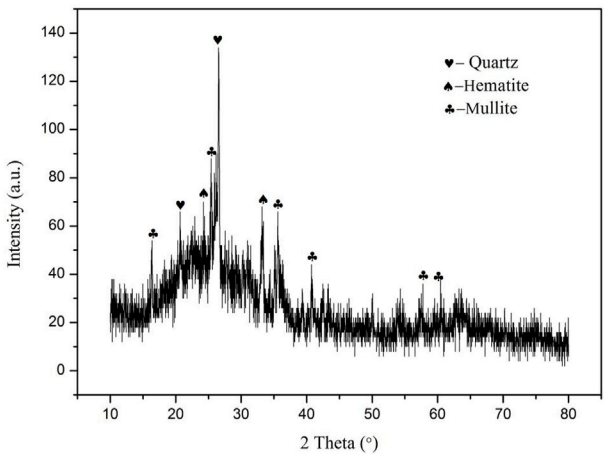

FIGURE 1
XRD pattern of FA.

mainly composed of vitreous body and also contains a certain amount of mineral crystals. The process mineralogy properties of these components have a great influence on the properties of glass ceramics prepared from fly ash.

3.2 Influence of quartz sand content

3.2.1 Surface morphology

Figure 2 show the digital photographs of sintered samples. Figures 2A–D represent the sintered samples (labled GFA1-GFA4) with QS content of 20wt%, 15wt%, 10wt% and 5wt% in the glaze paste formula, respectively. Figure 2E represents the sintered body. Clearly, the glaze layers are perfectly fitting on the green bodies, and all samples show good opalescence and strong covering ability. However, the opalescence effect of samples first increased and then decreased with the increase of quartz sand content, which is because the quartz sand content affects the high temperature viscosity and sintering temperature of the glaze layer. Under the condition of a certain temperature, the higher the content of quartz sand is, the higher the viscosity of the glaze layer is, and the worse the melting property is. Obviously, GFA1 has a thick glaze layer due to poor melting. And, the surface presents obvious stress cracks, which is due to the high content of quartz sand, resulting in high Si/O radio in the glaze, so that the silicon-oxygen tetrahedral network connection in the glaze layer is strong, which improves the elastic modulus of the glaze layer, and then reduces the elasticity of the glaze layer, so it is easy to appear stress-

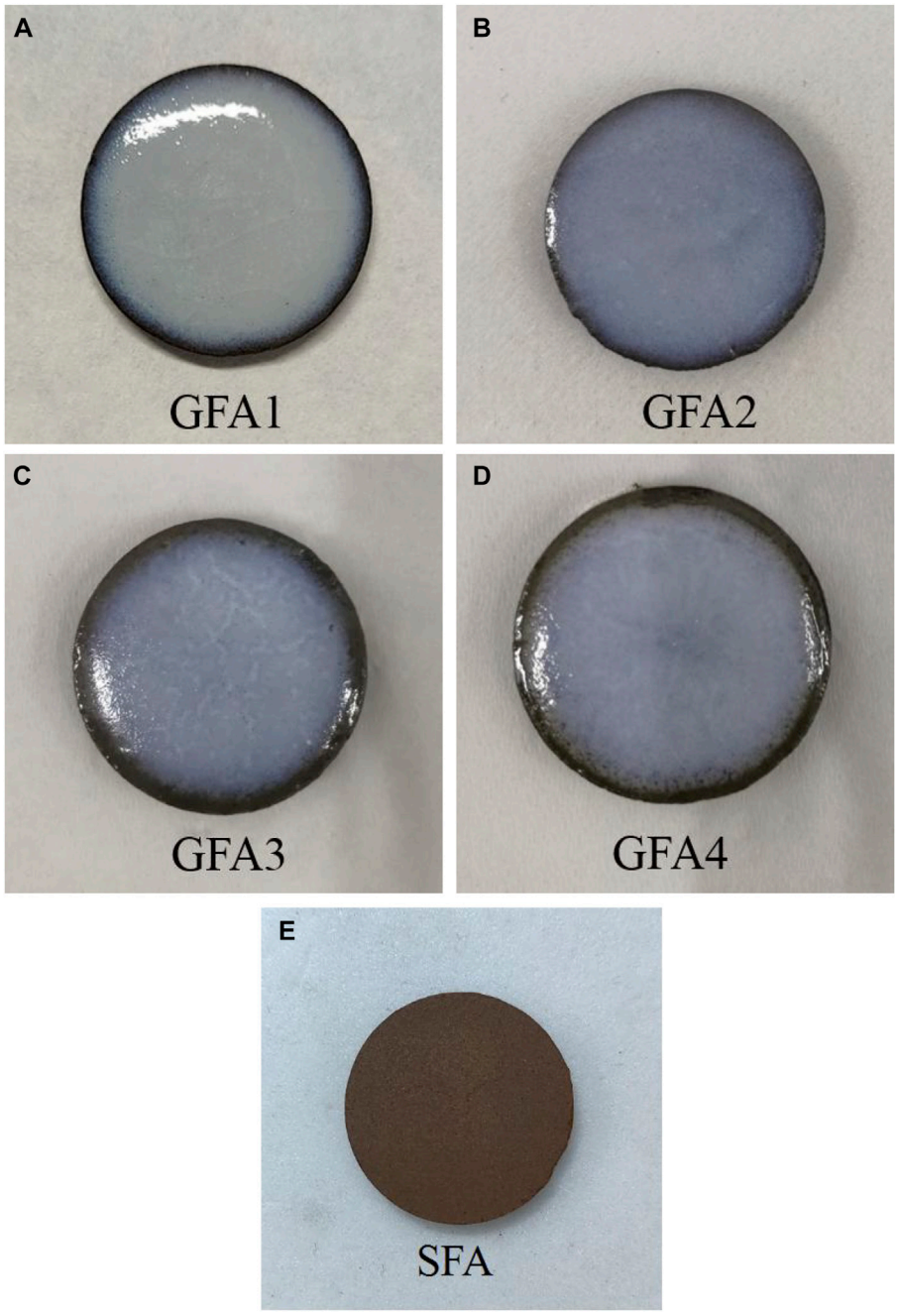

FIGURE 2
The digital photos of sintered samples ((**A**)-GFA1-20wt% QS, (**B**)-GFA2-15wt% QS, (**C**)-GFA3-10wt% QS, (**D**)-5wt% QS, (**E**)-sintered body).

generated defects. Due to lower quartz sand content, which is resulted in low glaze viscosity, so the edges of samples GFA3 and GFA4 show dry glaze phenomenon. The surface of GFA2 is flat and smooth, and has a good coverage effect. This indicates that the quartz sand addition has a great impact on surface morphology of sintered samples.

3.2.2 Phase analysis

Figure 3 shows the XRD patterns of glaze surface of samples with different QS contents (GFA1-GFA4). Clearly, anorthite (PDF # 00–002–0523, $CaAl_2$ $(SiO_4)_2$) and enstatite (PDF # 00–019–0768, $MgSiO_3$) phases can be detected in glaze surface of all samples, and the peak intensity of them decrease with increasing content of added QS. But, a faint augite (PDF # 00–024–0201, Ca (Fe, Mg) Si_2O_6) peak is only observed for samples GFA1 with 20 wt% added QS and GFA3 with 10 wt% QS. It can be also observed that no noticeable mullite (PDF # 00–002–0452, $3Al_2O_3!2SiO_2$) peak is detected in sample GFA4 with 5 wt% QS, it is first observed for sample GFA3 (10 wt% QS), and the peak intensity increases significantly with increasing content of added QS. Careful observation reveals the presence of a broad hump in the 2θ range between 15° and 35°, which indicates that the glass phase is formed during the sintering process. The bulge in the peak of the glass phase first gradually

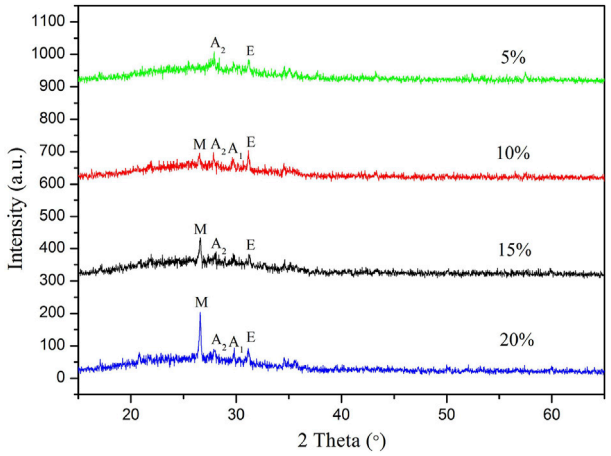

FIGURE 3
XRD patterns of glaze surface of samples with different QS contents: (M-Mullite, A_1-Augite, A_2-Anorthite, E-Enstatite).

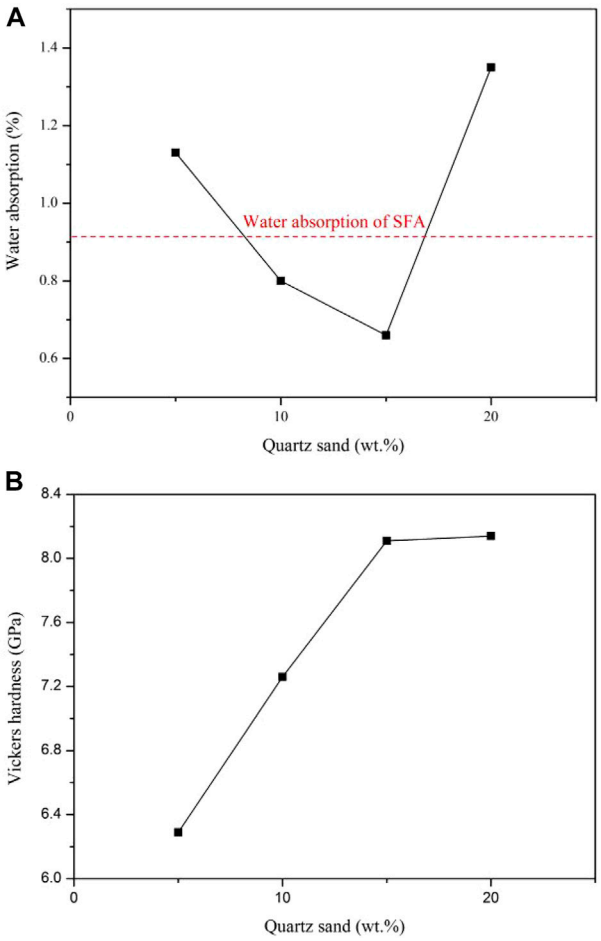

FIGURE 4
(A) Water absorption, **(B)** Vickers hardness of samples GFA1-GFA4.

increases with the QS addition, and then decreases when the QS content exceeds 15 wt%.

The glaze surface of sample GFA2 is mainly composed of mullite (PDF # 00–002–0452), in addition, the faint anorthite (PDF # 00–002–0523) and enstatite (00–019–0768) peaks can be observed. The above-mentioned phenomenon can be explained based on the fact that QS contains a large quantity of SiO_2 served as the glass network. At the beginning, the amount of QS was small, resulting in low SiO_2 content, while the relative content of CaO and MgO as network modifiers was high, which can effectively break the Si–O–Si bond of the quartz crystal from raw materials and increase the percentage of non-bridging oxygen ions. This results in the reduction in the [SiO_4] tetrahedral bonding strength and the increase in the content of amorphous SiO_2. The depolymerization of [SiO_4] tetrahedron reduces the viscosity of the liquid phase and increases the migration rate of Ca^{2+} and Mg^{2+} ions. The excess Ca^{2+} and Mg^{2+} ions combine with amorphous SiO_2 to promote the precipitation of the crystals such as enstatite, anorthite, et al., which is another reason for the observed low in the content of the glass phase. With the increase of QS dosage, SiO_2 content increases, and more silicon-oxygen tetrahedral volume is formed at high temperature, thus more and more glass phases are formed. At the same time, the mullite phase, which can increase the mechanical strength of the glaze, improve the hardness of the glaze, begins to appear and the peak becomes stronger.

3.2.3 Physical and mechanical properties

The influence of QS content on the physical and mechanical properties of the sintered complex is shown in Figure 4, in which the red imaginary horizontal line represents the water absorption of the sintered solid waste glass ceramic base body. Figures 4A,B demonstrate that the QS content is a turning point at 15wt%. From Figure 4A, it can be seen that water absorption of the complexes labeled GFA1-GFA4 first decrease and then increase with the increase in the QS content, and the minimum values are obtained at 15 wt%. Moreover, it is obvious that the water absorption of the complex is less than that of the sintered base body when the QS content is 10wt%-15wt%. Figure 4B shows with the increase in the QS content from 5 to 15 wt%, the Vickers hardness increases sharply, then does not change significantly. This indicates that the QS addition has a great impact on the glaze performance, which is related to the fluidity of the glaze after melting and the lubrication ability between the glaze and the base body, which are directly affected by the high temperature viscosity of the glaze. The glaze viscosity is first determined by the degree of silicon-oxygen tetrahedral network connection. The viscosity decreases with the increase of O/Si ratio. However, when the O/Si ratio increases, the large tetrahedral group will decompose into the small tetrahedral group. The connection between tetrahedra decreases, and the gap increases accordingly, resulting in the decrease of glaze melt viscosity. Small viscosity is prone to dry glaze, needle eye and other phenomena, resulting in large glaze water absorption. Large viscosity, easy to appear stress cracks and other defects, will also make the glaze water absorption increased. The hardness of glaze is mainly determined by the chemical composition, mineral composition and microstructure of glaze. Because SiO_2 that makes up the glass network will significantly improve the hardness of the glass, the glaze with high silicon content has high hardness. In addition, the precipitated microcrystals in the glaze layer are highly dispersed on the whole glaze, which will increase the hardness of the glaze

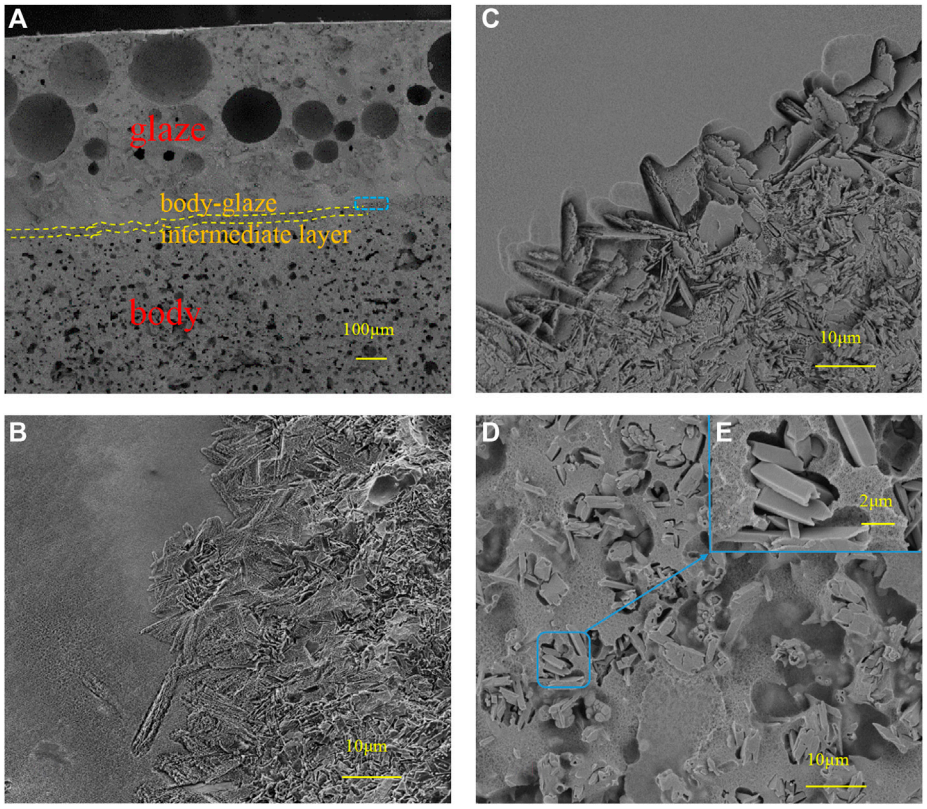

FIGURE 5
The SEM micrographs of the section **(A–C)** and glaze surface **(D,E)** of sample GFA2.

obviously (as shown in Figures 5D,E). However, the stress crack defect on the glaze surface caused by the high temperature viscosity of the glaze melt due to the high content of quartz sand, will accelerate the wear of the glaze layer and reduce the hardness of the glaze. Therefore, as the QS content exceeding 15%, the change of glaze hardness is not obvious.

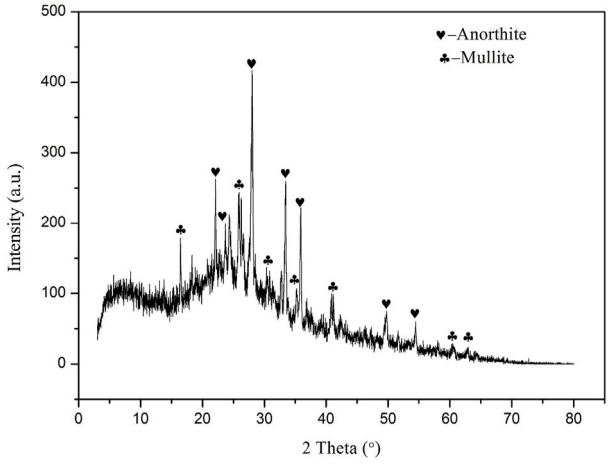

FIGURE 6
XRD pattern of body-glaze intermediate layer of sample GFA2.

3.3 Microstructure and phase analysis

Figure 5 illustrates the morphologies of the cross-section and glazed surface of the complex with 15wt% SiO_2 sintered at 1180 °C for 30 min. The cross-section image (Figure 5A) shows that the sintered complex can be divided into three parts: the base body at the bottom, the body-glaze intermediate layer (the part between the yellow dotted lines) in the middle and the top glazed layer. It can be seen that the glazed layer is about 500μm, which consists of three parts: the top thin layer has good compactness and is mainly distributed with crystal structures showed in Figure 5D, which can enhance the surface finish and the mechanical strength of products. Besides, these crystals will scatter light, lead to a good opalescence effect. The middle part is thicker and mainly contains pores of different sizes, which can also scatter light to form an opalescent effect. These reasons mentioned above play a role in covering the base body. In addition, the elastic modulus of the pore is close to zero, which can reduce the elastic modulus of the glaze and improve the thermal shock resistance of the product to a certain extent. The bottom part (near the body-glaze intermediate layer) has the best compactness and can be better fit with the crystal structure of the body-glaze intermediate layer. On the whole, the density of the glaze layer is obviously better than that of the base body, as shown in Figure 5B, which is the enlarged picture of the part marked with box in Figure 5A. The body is loose and has a high porosity, resulting in high water absorption after sintering. From Figure 5B, it can also be seen that the glaze layer and the body are closely connected together through the intermediate transition layer. Figure 5C shows an enlarged view of the part of the connection between the intermediate transition layer and the glaze layer after HF acid etching. Clearly, the glaze layer is dense. The

intermediate transition layer, composed of plate-like crystal structures doped with some columnar crystal structures (the phase analysis is shown in Figure 6), is pinned in the glaze layer. Combining with the XRD analysis in Figure 6, they are inferred as the mullite phase (PDF # 00–002–0415, $3Al_2O_3!2SiO_2$) and the anorthite phase (PDF # 00–002–0537, $Al_2Ca(SiO_4)_2$). In the process of high temperature sintering, these crystal structures are plate like, needle like, directly inserted into the molten glass phase of the glaze layer and the base body. After solidification, the crystal structures are inlaid between the two layers like nails, which enhances the binding of base body and glaze layer.

Figure 5D shows SEM of the glaze surface by HF acid etching. Careful observation reveals the presence of a honeycomb network structure and a large number of columnar crystals and irregular grain structures on the glaze surface, which indicates that the glass phase and a large amount of mullite phase and very little anorthite phase, are formed during the sintering process. These inferences can be verified in XRD (Figure 3). Figure 5E is an enlarged view of the part inside the blue box in Figure 5D, from which it can be seen that the diameter of columnar crystals varies from less than 1 μm to nearly 2μm, and most of them are between 1 and 2 μm. This is the reason why the glaze hardness increases, and can greatly enhance the mechanical strength of the body surface. However, the size of those irregular grain structures are in the hundreds of nanometers, the Rayleigh scattering might occur in glaze. And the glaze color formed is due to the structural color developed by the Rayleigh scattering, which occurs when the size range of the object is comparable to the optical wavelength(λ) range (Kinoshita and Yoshioka S, 2005; Higashiguchi et al., 2012). The smaller the λ, the easier the Rayleigh scattering. Since blue light is at the short wavelength end of the visible spectrum, it is scattered in the atmosphere much more than the longer-wavelength light. As a result, the structural color developed by the Rayleigh scattering shows that blue and the glaze colors become blue with addition of calcium phosphate (Yang et al., 2005). Hence, the glaze color of products is blue in this paper.

4 Conclusion

The blue opaque glazes perfectly fitting on the glass ceramic base body prepared from FA are produced. These products are sintered at 1180°C for 30 min. The optimal quartz sand content are selected as 15wt% through analyzing the relationship between the addition of quartz sand and quality of glaze surface appearance. The SEM microstructure shows that the irregular grain structures were developed in glazes and their sizes are in the hundreds of nanometers, so the structural color is formed owing to the Rayleigh scattering and the glaze color gets blue. In addition, columnar crystals are formed in the glaze layer, which are found to be mullite by the XRD analysis and improve the mechanical strength of the glaze layer. According to the physical and mechanical properties results, the water absorption of the product is .66%, which is lower than the absorption of the sintered solid waste glass-ceramics body of .93%. And the Vickers microhardness of the product is 8.1 GPa, which improves the mechanical properties of solid waste glass ceramic base body.

Data availability statement

The raw data supporting the conclusions of this article will be made available by the authors, without undue reservation.

Author contributions

HY and HG. performed the experimentals, analyzed the data, and writed manuscript. HS and TP guided the manuscript and corrected the manuscript.

Funding

This work was supported by the Science and Technology Project of Chongqing Municipal Commission of Education (No.KJQN202201441), the New Generation Information Technology Innovation Project(No. 2021ITA04001) and the Intellectual property special project of Sichuan Intellectual Property Office(No. 2022-ZS-00031).

Conflict of interest

The authors declare that the research was conducted in the absence of any commercial or financial relationships that could be construed as a potential conflict of interest.

Publisher's note

All claims expressed in this article are solely those of the authors and do not necessarily represent those of their affiliated organizations, or those of the publisher, the editors and the reviewers. Any product that may be evaluated in this article, or claim that may be made by its manufacturer, is not guaranteed or endorsed by the publisher.

References

Albertini, A. V. P., Silva, J. L., Freire, V. N., Santos, R., Martins, J., Cavada, B., et al. (2013). Immobilized invertase studies on glass–ceramic support from coal fly ashes. *Chem. Eng. J.* 214, 91–96. doi:10.1016/j.cej.2012.10.029

Ali, D., Sharma, U., Singh, R., and Singh, L. P. (2021). Impact of silica nanoparticles on the durability of fly ash concrete. *Front. Built Environ.* 7. doi:10.3389/fbuil.2021.665549

Barbieri, L., Lancellotti, I., Manfredini, T., Ignasi QueraltRincon, J., and Romero, M. (1999). Design, obtainment and properties of glasses and glass–ceramics from coal fly ash. *Fuel* 78 (2), 271–276. doi:10.1016/S0016-2361(98)00134-3

Dong, J. F., Huang, Z. H., Chen, B., Huang, J., Fang, M. H., Liu, Y. G., et al. (2009). Study on synthesis of spinel-sialon multiphase material from fly ash and aluminum dross in-situ reaction. *J. Synthetic Cryst.* 38 (1), 371–374.

Erol, M., Küçükbayrak, S., and Ersoy-Meriçboyu, A. (2008). Characterization of sintered coal fly ashes. *Fuel* 87 (7), 1334–1340. doi:10.1016/j.fuel.2007.07.002

Fernandes, H. R., Tulyaganov, D. U., and Ferreira, J. M. F. (2009). Preparation and characterization of foams from sheet glass and fly ash using carbonates as foaming agents. *Ceram. Int.* 35, 229–235. doi:10.1016/j.ceramint.2007.10.019

Gao, Y., Duan, K., Xiang, S., and Zeng, W. (2021). Basic properties of fly ash/slag -concrete slurry waste geopolymer activated by sodium carbonate and different silicon sources. *Front. Mat.* 8, 751585. doi:10.3389/fmats.2021.751585

Guo, Y. X., Zhang, Y. H., Huang, H. W., and Hu, P. (2014). Effect of heat treatment process on the preparation of foamed glass ceramic from red mud and fly ash. *Appl. Mech. Mat.* 670-671, 201–204. doi:10.4028/www.scientific.net/AMM.670-671.201

Higashiguchi, K., Inoue, M., Oda, T., and Matsuda, K. (2012). Solvent-responsive structural colored balloons. *Langmuir* 28, 5432–5437. doi:10.1021/la3006234

Iyer, R. S., and Scott, J. A. (2001). Power station fly ash–a review of value-added utilization outside of the construction industry. *Resour. Conservation Recycl.* 31, 217–228. doi:10.1016/S0921-3449(00)00084-7

Kinoshita, S., and Yoshioka, S. (2005). Structural colors in nature: The role of regularity and irregularity in the structure. *Chem. Phys. Chem.* 6, 1442–1459. doi:10.1002/cphc.200500007

Li, B. W., Deng, L. B., Zhang, X. F., and Xiaolin, J. (2013). Structure and performance of glass–ceramics obtained by Bayan Obo tailing and fly ash. *J.Non-Cryst. Solid.* 380, 103–108. doi:10.1016/j.jnoncrysol.2013.09.012

Lu, Z., Lu, J., Li, X., and Shao, G. (2016). Effect of MgO addition on sinterability, crystallization kinetics, and flexural strength of glass–ceramics from waste materials. *Ceram. Int.* 42 (2), 3452–3459. doi:10.1016/j.ceramint.2015.10.142

Shang, W., Peng, Z., Xu, F., Tang, H., Jiang, T., Li, G., et al. (2021). Preparation of enstatite-spinel based glass-ceramics by co-utilization of ferronickel slag and coal fly ash. *Ceram. Int.* 47 (3), 29400–29409. doi:10.1016/j.ceramint.2021.07.108

Wang, S. M., Zhang, C. X., and Chen, J. D. (2014). Utilization of coal fly ash for the production of glass-ceramics with unique performances: A brief review. *J. Mat. Sci. Technol.* 30 (12), 1208–1212. doi:10.1016/j.jmst.2014.10.005

Yang, S. M., and Zhang, W. (2015). Research on glass ceramics of multi-solid waste slag by blast furnace slag and fly ash. *Bull. Chin. Ceram. Soc.* 34 (2), 487–491.

Yang, Y., Min, F., Xue, L., Mao, Z., Wang, C., Sun, X., et al. (2005). Microstructural analysis of the color-generating mechanism in ru ware, modern copies and its differentiation with jun ware. *J. Archaeol. Sci.* 32, 301–310. doi:10.1016/j.jas.2004.09.007

Zhang, J., Zhang, X., Liu, B., Ekberg, C., Zhao, S., and Zhang, S. (2022). Phase evolution and properties of glass ceramic foams prepared by bottom ash, fly ash and pickling sludge. *J. Mineral Metallurgy Mater.* 29 (3), 563–573. doi:10.1007/s12613-020-2219-5

Zhang, Z., Wang, J., Liu, L., Ma, J., and Shen, B. (2020). Preparation of additive-free glass-ceramics from msw incineration bottom ash and coal fly ash. *Constr. Build. Mat.* 254, 119345. doi:10.1016/j.conbuildmat.2020.119345

Zhao, Y., Ye, J., Lu, X., Liu, M., Lin, Y., Gong, W., et al. (2010). Preparation of sintered foam materials by alkali-activated coal fly ash. *J. Hazard. Mater.* 174 (1-3), 108–112. doi:10.1016/j.jhazmat.2009.09.023

Zhu, M. G., Ji, R., Li, Z. M., Wang, H., Liu, L., and Zhang, Z. (2016). Preparation of glass ceramic foams for thermal insulation applications from coal fly ash and waste glass. *Constr. Build. Mat.* 112, 398–405. doi:10.1016/j.conbuildmat.2016.02.183